COLO HEP 402

Study of the Production of Supersymmetric Particles

Brook Williams

April 15, 1998

COLO HEP 402

Abstract

This is a study of how supersymmetry might be detected in a 500 GeV e^+e^-collider with an 80% right polarized electron beam. These parameters were chosen to be consistent with the proposed Next Linear Collider. In particular this thesis studies the production of charginos. One is able to separate the signal from the background and determine the masses of the chargino and neutralino. Furthermore, it can be shown that the error is minimized for a center of mass energy of 445 GeV.

Contents

1 Introduction

The unification of the weak and electromagnetic force during the 70's led to an exciting new era in particle physics. Due to this unification physicists were able to accurately predict the existence of new particles, such as the top quark, and make great strides in understanding what comprised the world in which we live. Physicists are now able to describe the world on a more fundamental level than ever before. This description is known as the Standard Model (Stdm). In the Standard Model there are two different classes of fundamental particles: fermions and bosons. The first class, fermions, make up "bulk matter" and can be further subdivided into two groups: leptons and quarks. Leptons, such as the electron, can be observed alone but quarks always appear in groups forming particles such as protons and neutrons; these particles are called hadrons. Bosons transmit the forces that cause fermions to interact. These forces are the electromagnetic, weak and the strong force[1]. The Standard Model also predicts the existence of the scalar Higgs field; this field is necessary to have a gauge invariant theory with massive particles and is important in unifying the weak and electromagnetic force. There are currently many searches for the Higgs boson. We are now ready to make the next great stride in the understanding of particle physics.

There is a serious problem in the Standard Model. The determination of the scalar Higgs field mass has unphysical infinities; this is known as the quadratic mass divergence. Physicists are currently investigating how one might correct these infinities. One proposed solution is called Supersymmetry (SUSY). In addition to canceling these infinities Supersymmetry causes the coupling constants[2] to have approximately the same value at a particular high energy, $\sim 10^{14}$ GeV. This is important when trying to unify the forces in nature. The unification of all the forces would create a simpler, more complete description of nature and is one of the ultimate goals in high energy physics. It also has been suggested that the lightest supersymmetric particle may account for the missing mass or "dark matter" in our universe. The observation of Supersymmetry will take us far beyond the understanding of the Standard Model and into the next era of particle physics. This thesis is the study of how SUSY may be detected in a 500 GeV e^+e^-collider.

[1] *It is thought that gravity is also transmitted by bosons and may one day be included in the Standard Model*

[2] *The coupling constants, which are not constants since they depend on the energy of the interaction taking place, represent the strengths of the 3 forces.*

In Supersymmetric theory for each "ordinary" particle there exists a superpartner whose spin differs by half an integer of Plank's constant ($\hbar$). Spin describes the intrinsic angular momentum of a particle. Fermions have a spin that is equal to half integer units of $\hbar$ and bosons have a spin that is equal to integer units of $\hbar$. If SUSY exists then for each particle there is both a fermion and a boson. Thus the addition of supersymmetric particles to the Standard Model creates a symmetry between fermions and bosons. Some models of SUSY also assume "R-parity" conservation in order to agree with experimental observations, such as the lack of proton decay. R-parity assigns a ± 1 quantum number to sparticles[3] and 0 to Standard Model particles. If R-parity is conserved in a reaction where two Standard Model particles produce supersymmetric particles the sparticles must be produced in pairs; one sparticle with R-parity equal to +1 and one with R-parity equal to -1 so that the total R-parity is still 0. This also implies that if a supersymmetric particle decays it must decay into another sparticle with the same R-parity and Standard Model particles. Therefore the lightest supersymmetric particle (LSP[4]) must be stable; if not the particle would then have to decay into a lighter supersymmetric particle which does not exist. Supersymmetric particles interact weakly with ordinary matter and they have, except for the LSP, a very short lifetime. So when a supersymmetric particle is produced it quickly decays into the LSP and "ordinary" matter. The LSP will not be detected and the supersymmetric event has the "signature" of missing energy[5]. By looking for this "signature" physicists are hoping to find evidence for SUSY. Since the LSP is not observable it may account for the dark matter in the universe.

2 SUSY Events

Supersymmetry might arise in many different forms. Since it is not possible at this point to determine which of these forms exists, it becomes necessary to study more than one set of parameters. The Minimal Supersymmetric Model, (MSSM), are SUSY models which require minimum change to the Standard Model. The MSSM does not specify relationships between

[3] *A sparticle is a supersymmetric particle*

[4] *In the model we are simulating the LSP is called the neutralino and is represented by* $\tilde{\chi}_1^0$

[5] *Since* $E = mc^2$ *missing mass and momentum are equivalent to missing energy.*

its parameters and thus makes no prediction of sparticle masses. In attempt to include gravity in Supersymmetry, Supergravity or SUGRA models, have put constraints on the relationships between parameters and have made it possible to predict sparticle masses from them. For Minimal Supergravity (mSUGRA) models there are four defining parameters:

- $\boldsymbol{m_0}$, the universal scalar mass
- $\boldsymbol{m_{1/2}}$, the universal gaugino mass
- $\boldsymbol{\tan\beta}$, the ratio of the Higgs field vacuum expectation value
- $\boldsymbol{sgn(\mu)}$, the sign of the SUSY conserving Higgsino mixing term $\boldsymbol{\mu}$

Five SUSY sets of values for these parameters have been chosen for this study. These five sets of values were chosen by a group of theorist during a meeting of High Energy physicists at Snowmass 1996[6]. They are shown

Table 1: Parameter Points.

	m_0	$m_{1/2}$	A_0	$\tan\beta$	$sgn(\mu)$		production
Point 1	400	200	0	2	-1		*dominantly chargino*
Point 2	100	300	0	2	-1		*dominantly selectron*
Point 3	200	100	0	2	-1		*mixed chargino/selectron/sneutrino*
Point 5	300	130	-600	2	+1		*includes top squarks*
	$m_{\tilde{g}}$	$m_{\tilde{q}}$	$m_{\tilde{\ell}_i}$	$\tan\beta$	μ	m_A	production
Point 4	900	1000	1000	10	-100	200	*heavy, pseudo-scalar and charged Higgs production is accessible. Point 4 is a non-supergravity (non-SUGRA) point.*

[6]Report of the Supersymmetry Theory Subgroup; from "New Directions for High Energy Physics: Proceedings of the 1996 DPF/DPB Summer Study on High Energy Physics" 1997

in table 1. Four of the parameter sets, (1-3,5), are part of the mSUGRA model. Point 4 has a different set of parameters outside of the mSUGRA model which gives rise to more massive sparticles. Each of these five sets emphasizes the production of different supersymmetric particles and different masses for these sparticles.

Table 2: Supersymmetric Particle Masses (GeV).

	Point 1	Point 2	Point 3	Point 4	Point 5
$\widetilde{\chi}_1^0$	86.050	128.702	44.519	77.834	57.174
$\widetilde{\chi}_2^0$	175.451	257.218	96.998	115.291	111.459
$\widetilde{\chi}_3^0$	492.790	535.721	257.063	146.844	444.800
$\widetilde{\chi}_4^0$	501.853	542.758	273.757	292.407	464.631
$\widetilde{\chi}_1^\pm$	175.366	257.200	96.384	96.056	110.104
$\widetilde{\chi}_2^\pm$	500.898	542.463	257.063	292.457	461.631
h^0	83.254	89.919	68.287	126.957	101.419
H^0	745.465	681.879	379.217	201.056	622.512
A^0	741.215	676.893	371.321	200.000	619.908
$\mathrm{H}^\pm$	744.783	680.812	378.714	214.810	623.997
$\widetilde{q}_L$	603.273	668.380	316.728	1000.000	462.488
$\widetilde{b}_L$	520.573	621.862	274.269	1000.000	380.759
$\widetilde{t}_1$	424.437	535.830	263.725	924.844	150.651
$\widetilde{q}_R$	603.237	668.380	316.728	1000.000	462.488
$\widetilde{b}_R$	595.553	653.097	312.965	1000.000	456.583
$\widetilde{t}_2$	550.603	656.470	329.466	1096.285	494.730
$\widetilde{\ell}_L^-$	425.922	238.213	215.704	1000.000	320.641
$\widetilde{\nu}_L$	421.395	230.022	206.622	1000.000	314.603
$\widetilde{\ell}_R^-$	408.796	156.952	206.543	1000.000	307.449
$\widetilde{g}$	550.616	759.035	298.401	900.000	425.521

Table 2 shows the sparticle masses for the 5 different points. The theoretical structure of SUSY and the masses for a particular point help determine what the cross sections and decay branching ratios are for that point.

With the many different possible combinations of parameter points, production modes and decay modes it becomes necessary to limit our study to one at a time. Our high energy physics group is studying all five parameter

Table 3: **Point 1:** Prod. modes and Cross sections at 500 GeV (80% right hand pol.)

Particles	Cross-section (fb)[7]	Production fraction
$\tilde{\chi}_1^+\tilde{\chi}_1^-$	132	39.9%
$\tilde{\chi}_1^0\tilde{\chi}_1^0$	122	36.9%
h^0Z^0	58	17.5%
$\tilde{\chi}_2^0\tilde{\chi}_1^0$	10	3.0%
$\tilde{\chi}_2^0\tilde{\chi}_2^0$	8	2.4%

points. This paper covers the study of point 1. In particular this paper studies the production mode $e^+ + e^- \Rightarrow \tilde{\chi}_1^+ + \tilde{\chi}_1^-$. As table 3 and figure 1 indicate

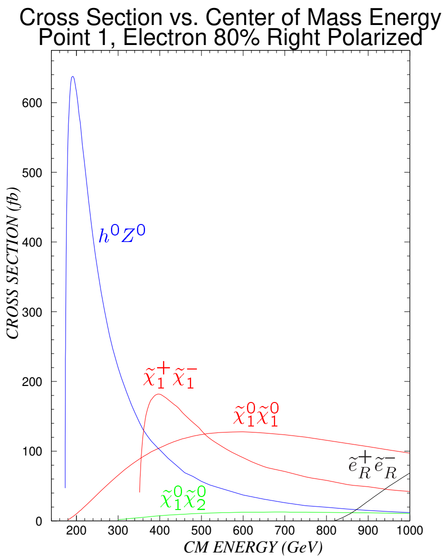

Figure 1: Dependence of the Cross section on Energy: Point 1

this mode has the largest cross section in point 1 at 500 GeV. Figure 1 show how the cross sections depend on the center of mass energy of the event. For an e^+e^-collision many of the production modes are highly dependent on the polarization of the incident electron as well. A particle is right polarized if its spin points in the direction of its motion and left polarized if its spin points opposite its direction of motion. A beam with 80% right handed polarization is a beam in which 80% of the particles are right polarized. Figure

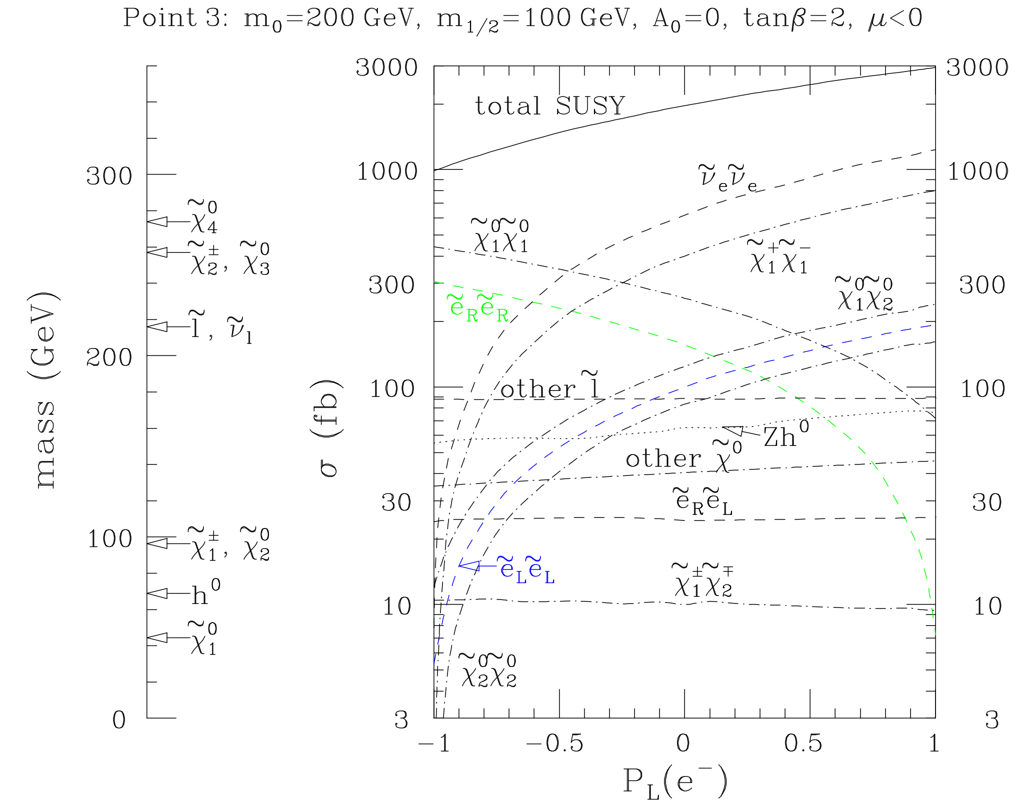

Figure 2: Dependence of the Cross section on Polarization: Point 3

2 shows for point 3, how SUSY's production modes depend on polarization. Eventually in our study we are going to use the cross-sectional dependence on polarization and $\sqrt{s}$ to optimize our results.

In the case of point 1, when the charginos decay, (99.8% of the time), a $\tilde{\chi}_1^0$ and a $W^\pm$ are produced. The $\tilde{\chi}_1^0$ is stable but the $W^\pm$ decays further. As you can see from table 4, 33% of the time when a $W^\pm$ decays, a neutrino

Table 4: $W^{\pm}$ **Branching ratios**

mode	**fraction**
$q\overline{q} \rightarrow hadrons$	67%
$l + \nu$	33%
$e^{\pm} + \nu_e(\overline{\nu}_e)$	11%
$\mu^{\pm} + \nu_\mu(\overline{\nu}_\mu)$	11%
$\tau^{\pm} + \nu_\tau(\overline{\nu}_\tau)$	11%

is produced. Because the neutrino escapes detection, energy is lost. When such an event occurs one is unable to determine how much energy is carried away by the $\tilde{\chi}_1^0$ making analysis of the event more difficult. Furthermore, the Standard Model process where $W^{\pm} \Rightarrow l + \nu$ can mimic these events making it hard to distinguish between Standard Model and SUSY events. For this reason this study has further been limited to events where the $W^{\pm}$ decays into hadrons, $W^{\pm} \Rightarrow q\overline{q}$[8]. Therefore, events where the series of processes,

$$e^+ + e^- \Rightarrow \tilde{\chi}_1^+ + \tilde{\chi}_1^- \text{ ...then...}$$
$$\tilde{\chi}_1^{\pm} \Rightarrow W^{\pm} + \tilde{\chi}_1^0 \text{ ...and...}$$
$$W^{\pm} \rightarrow q\overline{q}$$

take place will be considered "signal" events, (see figure 3). All other SUSY events along with any Standard Model events will be considered "background".

By studying the kinematical differences between "signal" and "background" events one is able to develop a method which separates the "signal" from the "background". To do this it is necessary to make a series of "cuts." A "cut" is when we throw out events that appear to be background so that the SUSY signal becomes more obvious.

I have been using the computer simulation programs, ISAJET and PYTHIA, to study how SUSY events would appear if supersymmetric particles were produced in a 500 GeV electron-positron collision. A center of mass energy of 500 GeV has been chosen because it is large enough to produce sparticles for most of the points. If these particles are seen at 500 GeV the energy

[8] $q\overline{q}$ - *quark anti-quark pair which form hadrons*

Figure 3: Feynman diagrams for the reaction $e^+ + e^- \Rightarrow \tilde{\chi}_1^+ + \tilde{\chi}_1^-$ ...then... $\tilde{\chi}_1^\pm \Rightarrow W^\pm + \tilde{\chi}_1^0$ ...and... $W^\pm \rightarrow q\overline{q}$. (Through the annihilation into a γ or a Z^0 (left) or through the exchange of a $\tilde{\nu}$ (right). The exchange of a $\tilde{\nu}$ is the more important diagram.

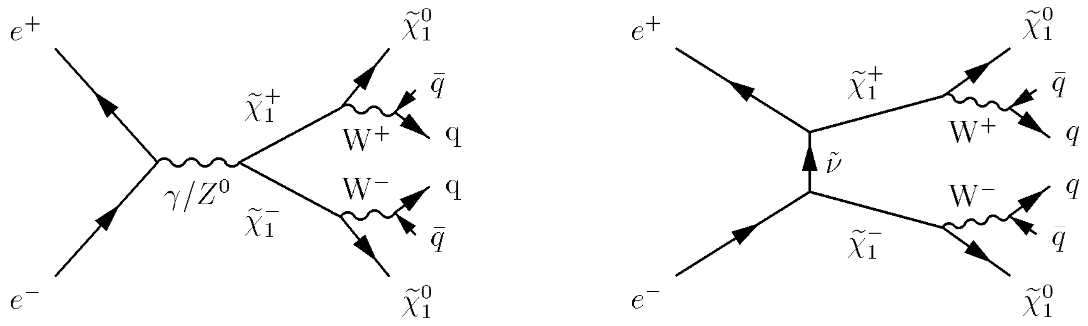

will be varied to enhance the production of these particles. ISAJET includes the possibility of polarizing the electron beam. Since the cross section of SUSY events and Standard Model events where $e^+ + e^- \Rightarrow W^+ + W^-$have a large dependence on the polarization of the beam, ISAJET was used in their simulation. On the other hand most other Standard Model processes have little dependence on the polarization. PYTHIA was used in the simulation of the rest of the Standard Model background because it is able to simulate a broader range of Standard Model processes. The simulation was for a 500 GeV electron-positron collider with 80% right handed polarization. These parameters are consistent with those for the proposed Next Linear Collider, NLC[9], which could help determine whether Supersymmetry exists.

3 Cuts

Chargino production through the exchange of a sneutrino, $\tilde{\nu}$, has the highest cross section. As you can see from table 2 the mass of the $\tilde{\nu}$ is 421.4 GeV for point 1. However, Standard Model events often take place through the exchange of particles such as γ, ν or Z^0. The heaviest of these particles, the Z^0, is 91 GeV. Because the mediator for chargino production is often

[9] *NLC is a proposed e^+e^- collider with a center of mass energy of 0.5 - 1.0 TeV.*

much heavier than the mediators for Standard Model events the cross section for $e^+ + e^- \Rightarrow \tilde{\chi}_1^+ + \tilde{\chi}_1^-$ is much smaller than many Standard Model cross sections. Figure 4 illustrates this difference in cross sections. The bottom histogram, (solid line), is what would be observed if supersymmetric and Standard Model events were being produced in the lab environment. The dashed line represents the events which are only part of the signal. For 50 fb^{-1} of data this signal contains only 2830 events while there are over one million total observed events. If we want to determine whether supersymmetric events are occurring we must improve this signal to background ratio dramatically. We describe below a series of cuts which improve the signal to background ratio.

3.1 Cut 1

A common Standard Model production mode is $e^+ + e^- \Rightarrow Z^0 + Z^0$. Some possible decay modes for the Z^0 are:

$$Z^0 \Rightarrow q\overline{q} \tag{1}$$
$$Z^0 \Rightarrow \nu\overline{\nu} \tag{2}$$

If both Z^0s decay as in (1) the quarks will hadronize and most of energy in the event will be detected. On the other hand if both Z^0s decay as in (2) the event will go completely undetected. But if one of the Z^0s decays as in (1) and the other decays as in (2), only the visible energy will come from the Z^0 which decayed into $q\overline{q}$. Since you lose all the energy from the Z^0 which decays into neutrinos your total visible energy for that event will be around $\frac{1}{2}$ the center of mass energy, which is 250 GeV. In figure 4 notice that the top-right histogram has a peak around 250 GeV. These events are due to this process. Since there is no energy deposited on the side of the event where $Z^0 \Rightarrow \nu\bar{\nu}$, energy in the backward hemisphere[10] is zero. Therefore by requiring that the total visible energy in the backward direction be greater than zero we are able to throw out these events.

Another common Stdm process is $e^+e^- \Rightarrow W^+ + W^-$. The decay where the $W^\pm$ decays into a lepton and a neutrino is also affected by this cut. In the center of mass frame of the $W^\pm$ momentum must be conserved. Therefore

[10] *The decays of the $W^\pm$ or $\tilde{\chi}_1^\pm$ form jets. These jets can be used to determine the "thrust axis," the axis defining the direction of "energy flow." The backward direction is defined as the side of the "thrust axis" with the least amount of energy.*

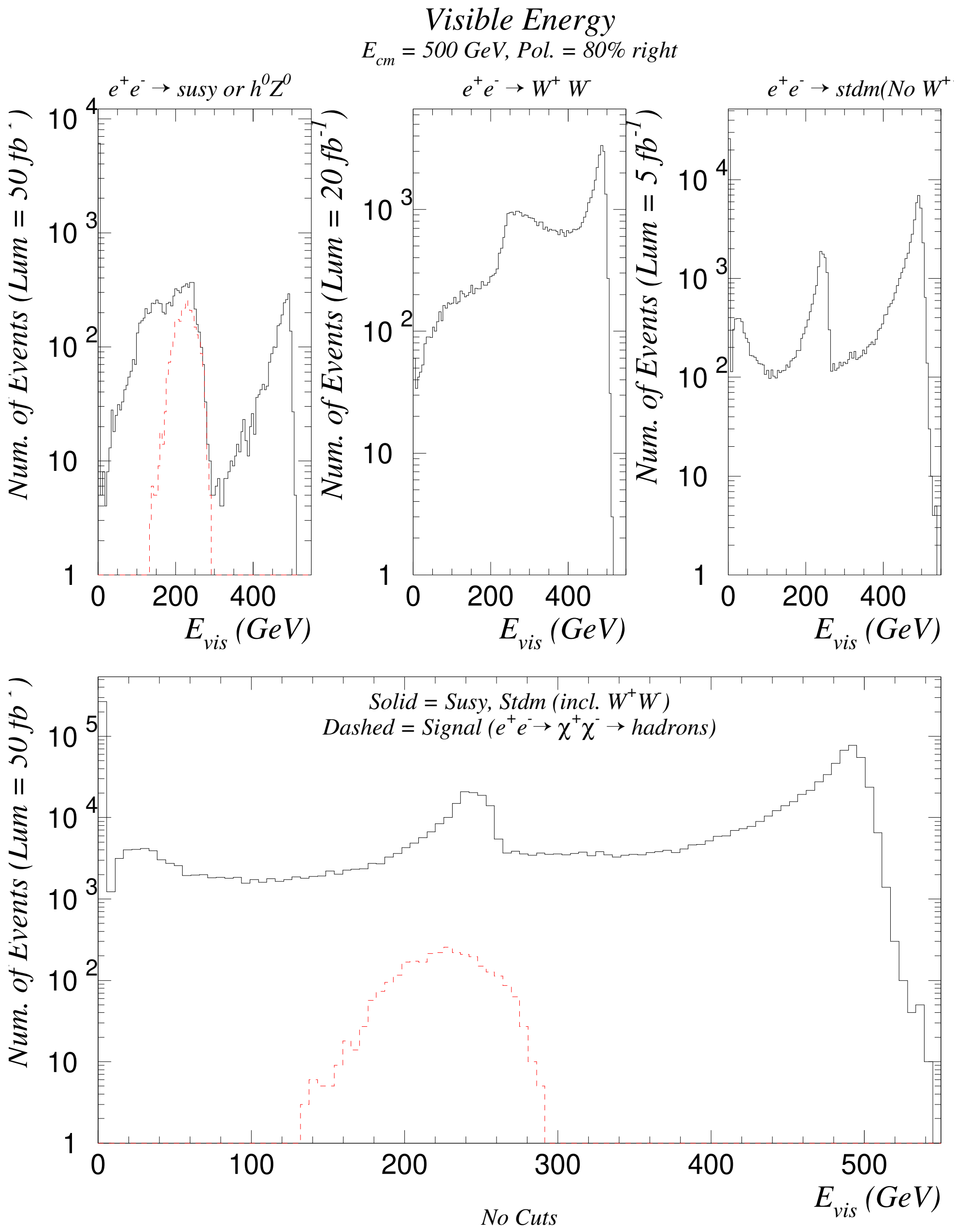

Figure 4: **Top left:** Solid Line - E_{vis} for SUSY & h^0Z^0 Dashed line - Signal **Top mid.:** E_{vis} for $e^+ + e^- \Rightarrow W^+ + W^-$ **Top right:** E_{vis} for Stdm events (except $W^\pm$) **Bottom:** Signal added to the background, the dashed line represents the signal alone.

the momentum of the neutrino must be equal to the momentum of the lepton. If the velocity of the neutrino is approximately in the same direction as the $W^{\pm}$ and the velocity of the lepton is opposite that of the $W^{\pm}$ the lepton becomes difficult to detect. That is because if we do a Lorentz transformation into the lab frame the lepton has very little momentum and therefore it often escapes detection. If the neutrino from the other $W^{\pm}$ decay is in the same direction as our low energy lepton it appears that there is no energy in the backward direction. This processes is much more common in $W^{\pm}$ decays than it is in chargino decays so by throwing out events that have zero visible energy in the backward direction we can again get rid of a large number of background events without losing much of the signal.

Figure 5 shows the data after requiring that the energy in the backward direction not be equal to zero. Notice how the peak at 250 GeV in the top right plot is no longer there. We have also lost about 3000 $W^{\pm}$ events.

3.2 Cut 2

If a Standard Model event does not contain neutrinos all the energy would be visible in a "perfect" detector. In a real detector some energy can be lost due to flaws in detectors, resolution and particles escaping down the beam pipe. In spite of these losses many Standard Model events have a visible energy which is close to the center of mass energy, 500 GeV. On the other hand energy is lost in all SUSY events due to the neutralinos escaping detection. In table 2 you can see that for point 1 the mass of the $\tilde{\chi}_1^0$ is 86.05 GeV. Therefore there is a minimum energy loss of 86.05 GeV in each hemisphere. In figure 6 you can see that the energy in the forward hemisphere[11] is peaked at just under 250 GeV. However the signal, (dashed line in the top histogram), has a sharp cut off around 170 GeV due to losing at least the mass of the neutralino. We can cut out events where most of the energy is detected by requiring that the energy in the forward hemisphere is less than or equal to $(\frac{1}{2} - 10\%)E_{cm}$. This allows for a 10% loss of energy due to detector flaws and resolution. Figure 7 shows the visible energy distribution after making this cut. Note that we have reduced the Standard Model background significantly without cutting into the signal. Also note that in figure 5 there is a large peak above 400 GeV. These events

[11] *The detector is divided into two hemispheres for each event. The "forward" hemisphere is the hemisphere in the forward direction as described in the previous footnote.*

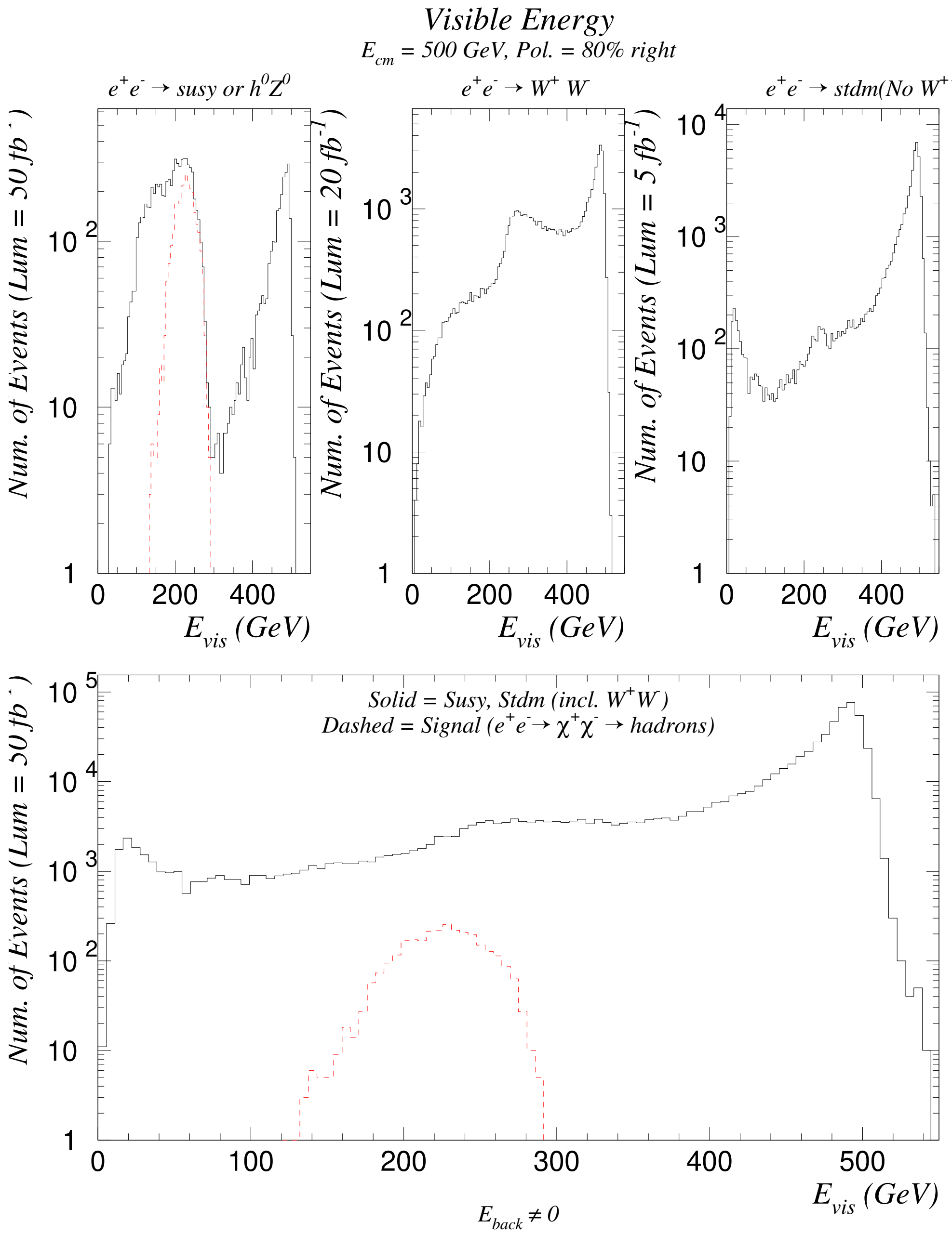

Figure 5: **Top left:** Solid Line - E_{vis} for SUSY & h^0Z^0 dashed line - Signal **Top mid.:** E_{vis} for $e^{+}+e^{-}\Rightarrow W^{+}+W^{-}$ **Top right:** E_{vis} for Stdm events (except $W^{\pm}$) **Bottom:** Signal added to the background, the dashed line represents the signal alone.

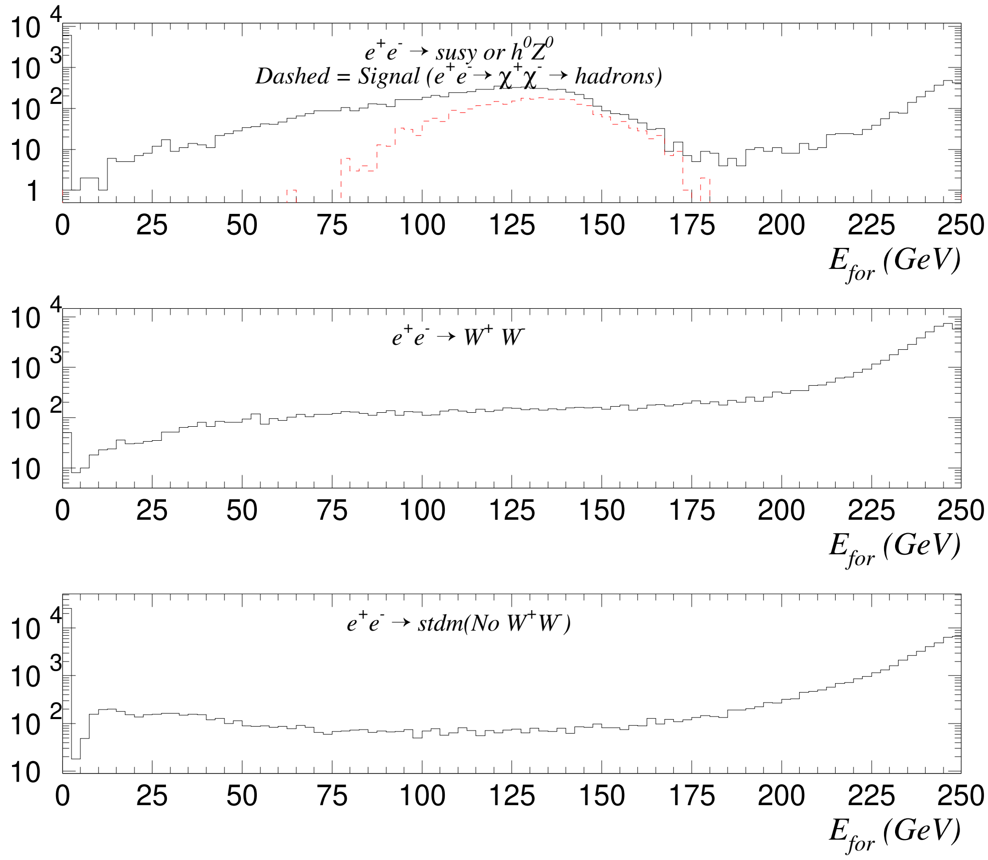

Figure 6: Energy in the forward hemisphere (GeV)

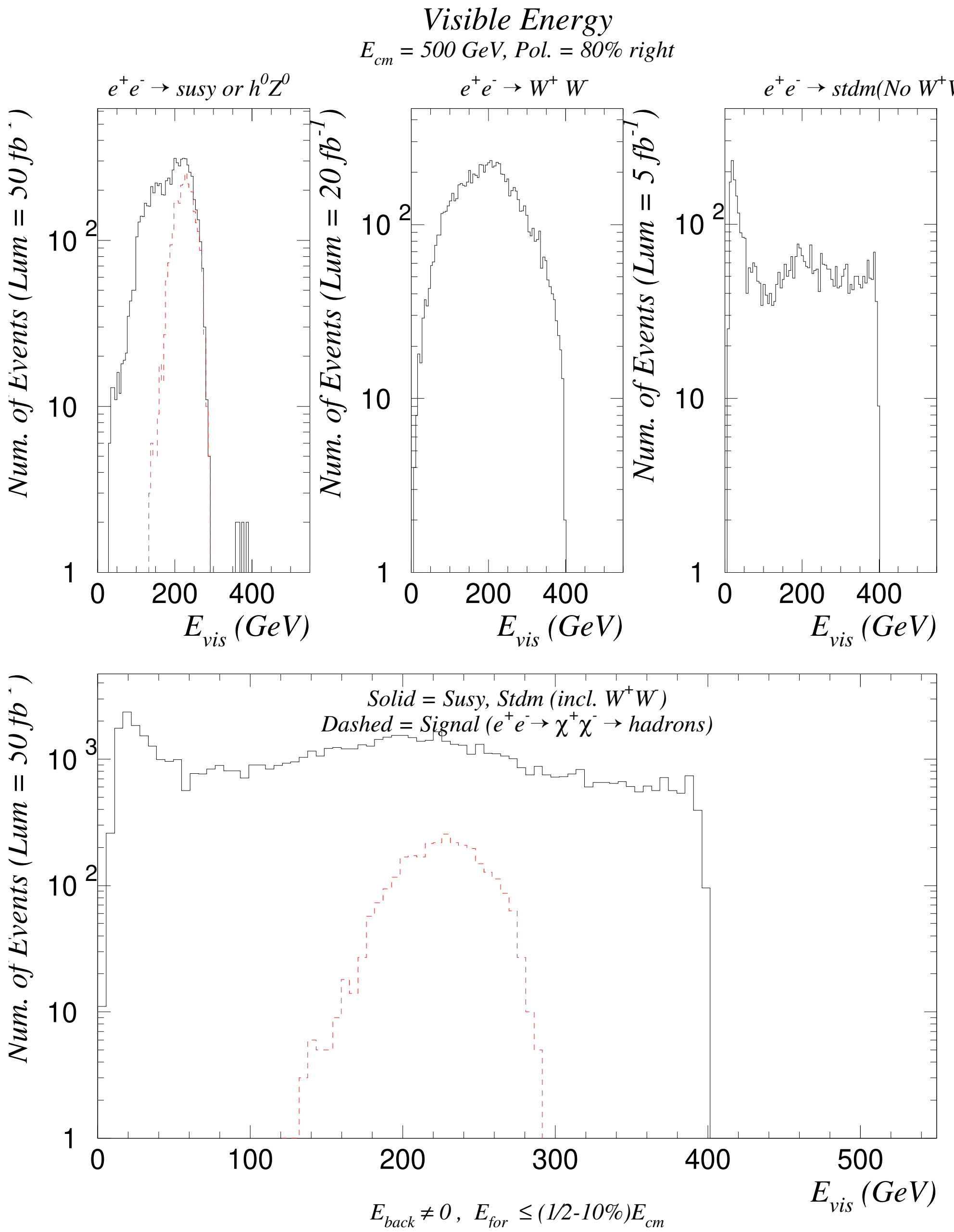

Figure 7: **Top left:** Solid Line - E$_{vis}$ for SUSY & h^0Z^0 Dashed line - Signal **Top mid.:** E$_{vis}$ for $e^+ + e^- \Rightarrow W^+ + W^-$ **Top right:** E$_{vis}$ for Stdm events (except $W^\pm$) **Top mid.:** E$_{vis}$ for $e^+ + e^- \Rightarrow W^+ + W^-$ **Top right:** E$_{vis}$ for Stdm events (except $W^\pm$) **Bottom:** Signal added to the background, the dashed line represents the signal alone.

are due to the process $e^+e^- \Rightarrow h^0Z^0$. Because no neutralinos are produced in this process, (the production of which requires a minimum energy loss of 172.1 GeV, twice the mass of the $\tilde{\chi}_1^0$), the visible energy is much higher than in SUSY events and therefore these events are also removed by Cut 2.

3.3 Cut 3

When events are very forward[12] much of the energy is lost down the beam pipe. This creates a problem in that the low visible energy[13] mimics the supersymmetric signal. By not keeping events where there is a high amount of energy deposited near the beam pipe we can get rid of most of these events. Of course many of our signal events are forward and therefore we do cut into our signal. This cut does however get rid of many more $W^{\pm}$ events than signal events. This is because when the reaction $e^+ + e^- \Rightarrow W^+ + W^-$ occurs the cross section is dependent on θ. How the cross section varies with θ depends on the mediator of the reaction. There are two ways in which the reaction might occur: the $e^{\pm}$ pair could annihilate into a Z^0, in this case the cross section goes as $\sim (1+\cos^2(\theta))$ but the more prevalent case is when the $e^{\pm}$ pair exchange a ν, in this case the cross section goes as $\sim 1/\sin^4(\theta/2)$. In either case the cross section is peaked in the forward direction; in the latter case it is peaked extremely forward. The cross section of SUSY events however is spread more evenly about $\cos\theta$. It can be seen in figure 8 that the signal is distributed fairly evenly over $\cos(\theta)$, while the background is extremely peaked in the forward direction, as expected. Therefore by requiring that the total energy in an event between $0.90 \leq \cos(\theta) \leq 0.99$ be less than 1 GeV we cut a much larger fraction of the $W^{\pm}$ background than the signal. The results of these cuts are shown in figure 9.

3.4 Cut 4

The SUSY events with neutrinos in them are not useful to us because the missing energy due to the neutrino will cause us problems when it comes time to determine the masses of the charginos. Since a lepton is produced with each neutrino we can use this to remove the events from the sample. Whenever a high energy, (above 1 GeV), $e^{\pm}$ or $\mu^{\pm}$ is detected we will remove

[12] *Events where most of the particles are at a small angle, θ, with respect to the beam pipe.*

[13] *Visible Energy: Energy which is seen by the detector*

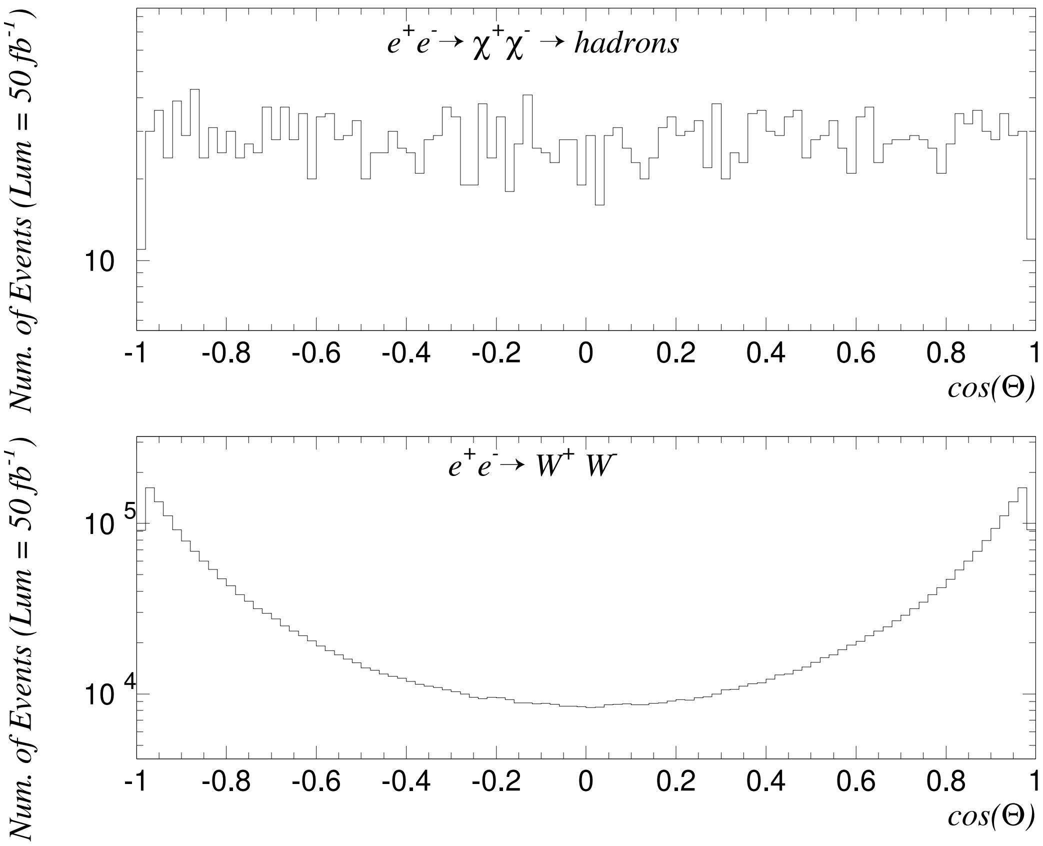

Figure 8: **Top:** $\cos(\theta)$ of Signal **Bottom:** $\cos(\theta)$ of $e^+ + e^- \Rightarrow W^+ + W^-$

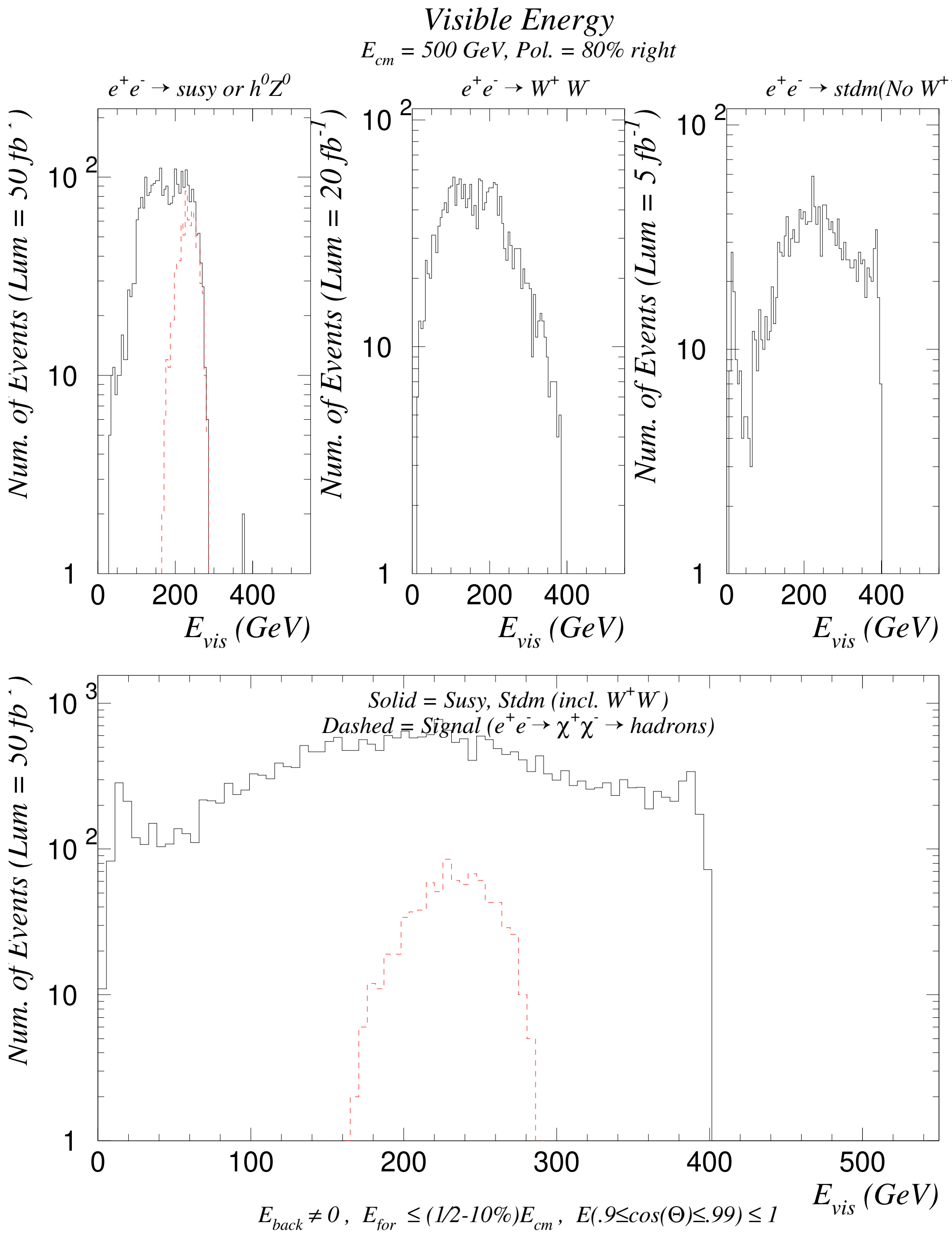

Figure 9: **Top left:** Solid Line - E_{vis} for SUSY & h^0Z^0 Dashed line - Signal **Top mid.:** E_{vis} for $e^+ + e^- \Rightarrow W^+ + W^-$ **Top right:** E_{vis} for Stdm events (except $W^\pm$) **Top mid.:** E_{vis} for $e^+ + e^- \Rightarrow W^+ + W^-$ **Top right:** E_{vis} for Stdm events (except $W^\pm$) **Bottom:** Signal added to the background, the dashed line represents the signal alone.

these events. We restrict it to high energy leptons because the low energy leptons probably come from secondary decays. These secondary decays will also have low energy neutrinos and will not affect the mass calculations very much. You can also see from Table 4 that these cuts should remove 22% of the background, assuming that we had perfect detectors. We did not cut out τ events because the lifetime of the τ is extremely short and therefore we can not directly detect the τ. However if the decays $\tau \to e + \nu_e$ or $\tau \to \mu + \nu_\mu$ occur these event will also be removed by this cut. Therefore the only τ events left are those in which $\tau \to hadrons$. By comparing figure 9 and figure 10 one can see how dramatically the $W^\pm$ background is affected by this cut.

3.5 Cut 5

As stated before our signal is,

$$e^+ + e^- \Rightarrow \tilde{\chi}_1^+ + \tilde{\chi}_1^- \text{ ...then...}$$
$$\tilde{\chi}_1^\pm \Rightarrow W^+ + W^- \text{...and...}$$
$$W^\pm \to q\overline{q}.$$

Each of the quarks then form jets. Since we have four quarks hadronizing we should, in principle, get four jets. If we then take two jets coming from the $q\overline{q}$ pair and find the combined mass of the two jets we should get the mass of the $W^\pm$. In real life it is often difficult to reconstruct jets and as always there is some energy loss which in turn affects the combined mass. One can find the two combinations of jets which give combined masses nearest the mass of the $W^\pm$, (M_W = 80.33 GeV)[14]. For a signal event there should be two good fits to the $W^\pm$ mass. Figure 11 shows that if one takes the second best fit and requires that its combined mass be greater than or equal to 60 GeV most of the remaining background is eliminated.

4 Results of the Cuts

There is a dramatic increase in our signal to background ratio from figure 4 to figure 11. Figure 12 is our data on a linear scale after all of the cuts. Almost all of the data are signal events. It is important though to see how the cuts affected our signal. Figure 13 shows that cut one and two do not

[14] *Particle Data Book, American Institute of Physics*

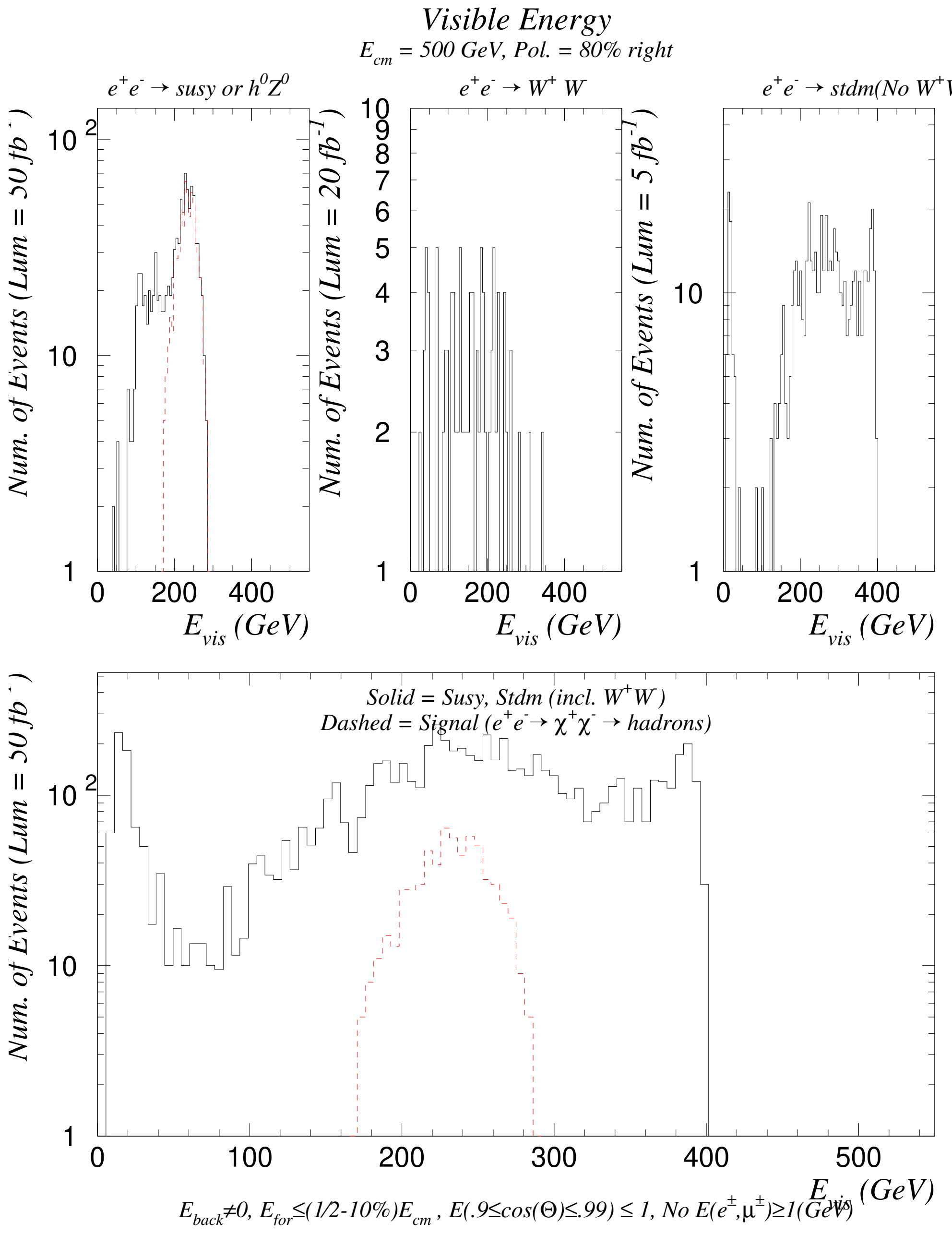

Figure 10: **Top left:** Solid Line - E_{vis} for SUSY & h^0Z^0 Dashed line - Signal **Top mid.:** E_{vis} for $e^+ + e^- \Rightarrow W^+ + W^-$ **Top right:** E_{vis} for Stdm events (except $W^{\pm}$) **Top mid.:** E_{vis} for $e^+ + e^- \Rightarrow W^+ + W^-$ **Top right:** E_{vis} for Stdm events (except $W^{\pm}$) **Bottom:** Signal added to the background, the dashed line represents the signal alone.

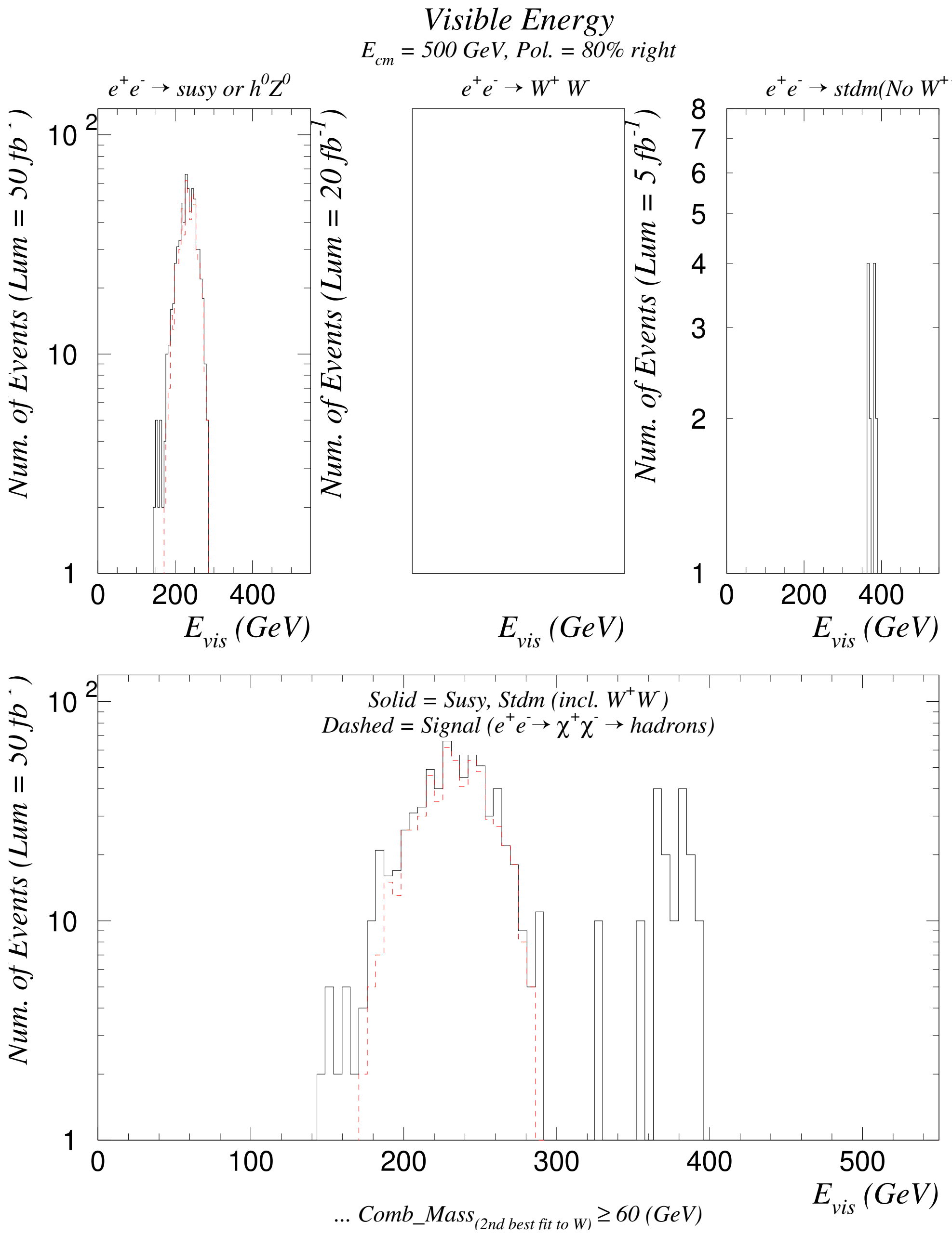

Figure 11: **Top left:** Solid Line - E_{vis} for SUSY & $h^0 Z^0$ Dashed line - Signal **Top mid.:** E_{vis} for $e^+ + e^- \Rightarrow W^+ + W^-$ **Top right:** E_{vis} for Stdm events (except $W^\pm$) **Top mid.:** E_{vis} for $e^+ + e^- \Rightarrow W^+ + W^-$ **Top right:** E_{vis} for Stdm events (except $W^\pm$) **Bottom:** Signal added to the background, the dashed line represents the signal alone.

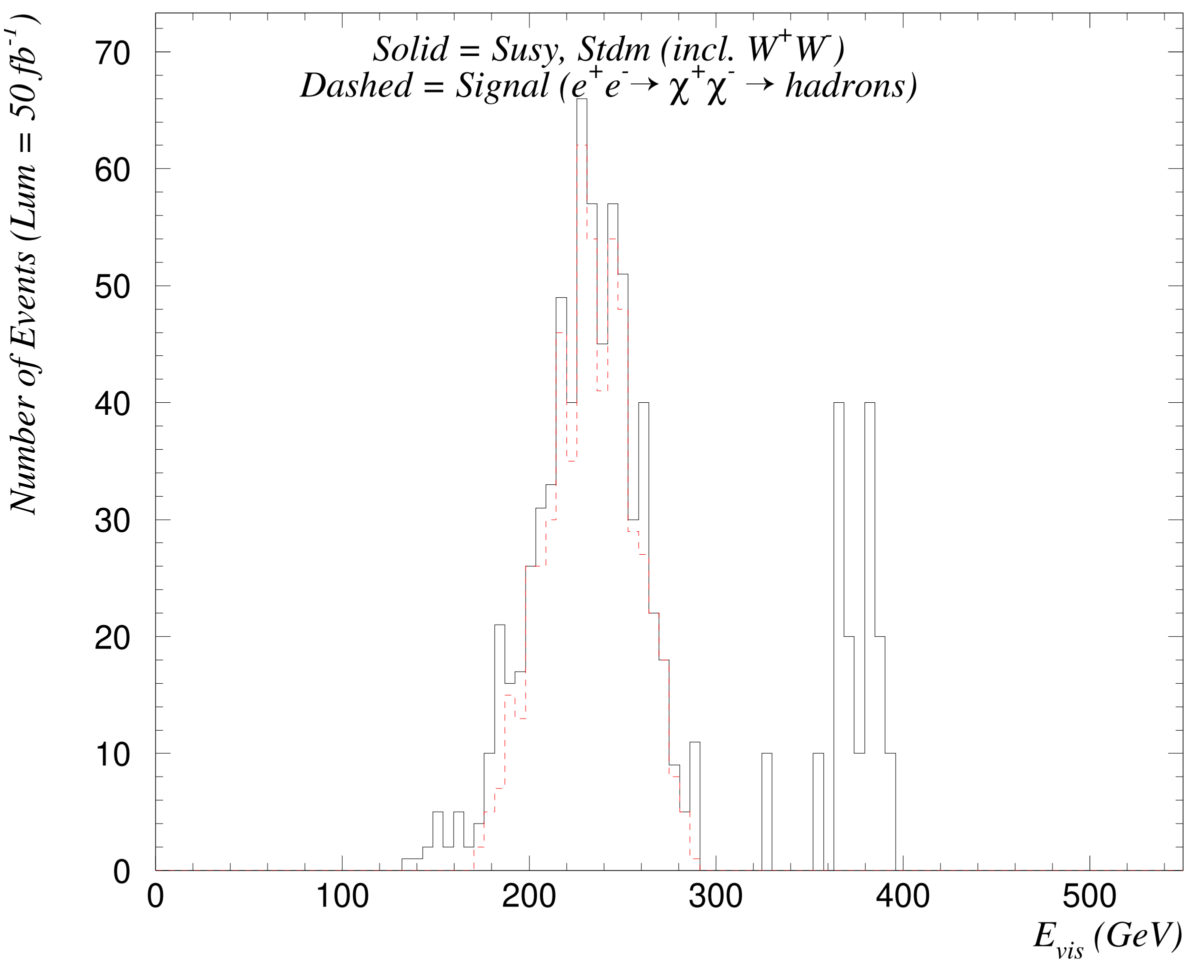

Figure 12: Visible energy after cuts

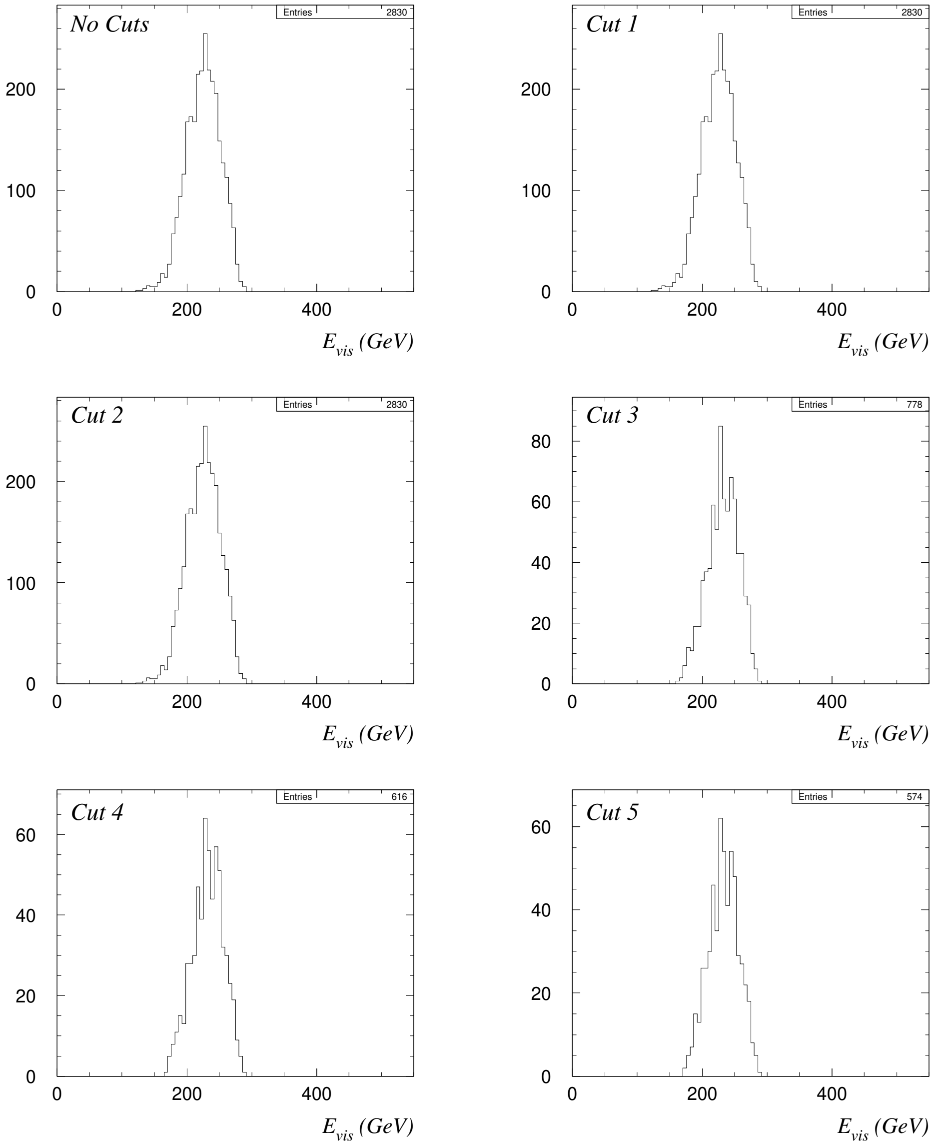

Figure 13: Visible energy of Signal

affect our signal at all. Cut three however cuts into our signal dramatically. Recall that cut three required that the visible energy between $0.90 \leq \cos(\theta) \leq 0.99$ be less than 1 GeV. This is an important cut because not only does it get rid of a large number of $W^{\pm}$ background but the events which it gets rid of are very similar in energy to that of the signal events. Since it is such an important cut it becomes necessary to ask if the cut just reduces statistics or does it affect the edges which become important during the analysis. Since the edges are relatively unaffected by cut three, the cut will be kept. Cuts four and five cut into the signal events by less than 20%.

Table 5: **Affect of Cuts on Signal**

Cut	**Num. of Events after Cuts**	**Percentage[a] of Signal lost**
None	2830	
1	2830	0%
2	2830	0%
3	778	73%
4	616	21%
5	574	7%
All	574	80%

[a] *Percentage of the signal remaining after the previous cut*

Table 5 summarizes how the cuts affected the signal. Although 80% of the signal was lost the edges were virtually unaffected. Because the edges were unaffected it is possible to now do the analysis and try to reconstruct the masses given in table 2.

5 Data Analysis

As previously stated the decay that is being investigated in this paper is,

$$\tilde{\chi}_1^{\pm} \Rightarrow \tilde{\chi}_1^0 + W^{\pm} \; .$$

Using the formulas derived in the appendix for a two body decay we can now reconstruct the masses of the $\tilde{\chi}_1^{\pm}$ and $\tilde{\chi}_1^0$. In a "perfect world" the masses we find would match exactly the masses given in table 2. Of course this is not the case in real life. It now becomes necessary to determine how close the measured masses agree with the initial parameters given in the simulation.

As explained in the description of **Cut 5** each jet is associated with a particular $W^{\pm}$. Figure 14 shows the combined mass for the best fit to the

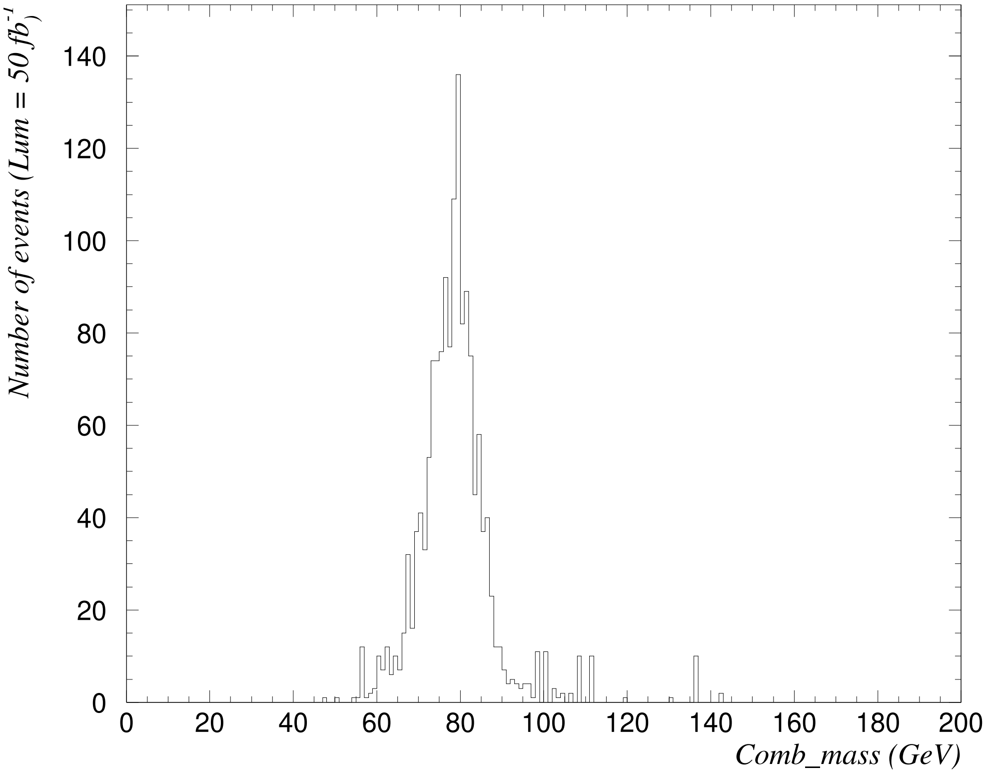

Figure 14: Combined masses of jets associated with a W

mass of the $W^{\pm}$. Notice that the histogram is peaked at 80 GeV, the mass of the $W^{\pm}$. The reason all of the events do not have a combined mass equal to the mass of the $W^{\pm}$ is once again due to measurement resolution problems and the reconstruction efficiency of detector. There are also a few left over background events which lead to a combined mass that is outside the gaussian centered at 80 GeV. The equations used in determining the masses of the $\tilde{\chi}_1^{\pm}$ and the $\tilde{\chi}_1^0$ depend on the maximum an minimum energy, as well as the mass, of the $W^{\pm}$. Therefore, the events where a substantial amount of energy is lost due to imperfections in the detector and events where the resolution leads to having too much or to little energy are not useful in determining the masses of the $\tilde{\chi}_1^{\pm}$ and the $\tilde{\chi}_1^0$. Thus, only events where the measured combined mass is 80±5 GeV are analyzed. Figure 15

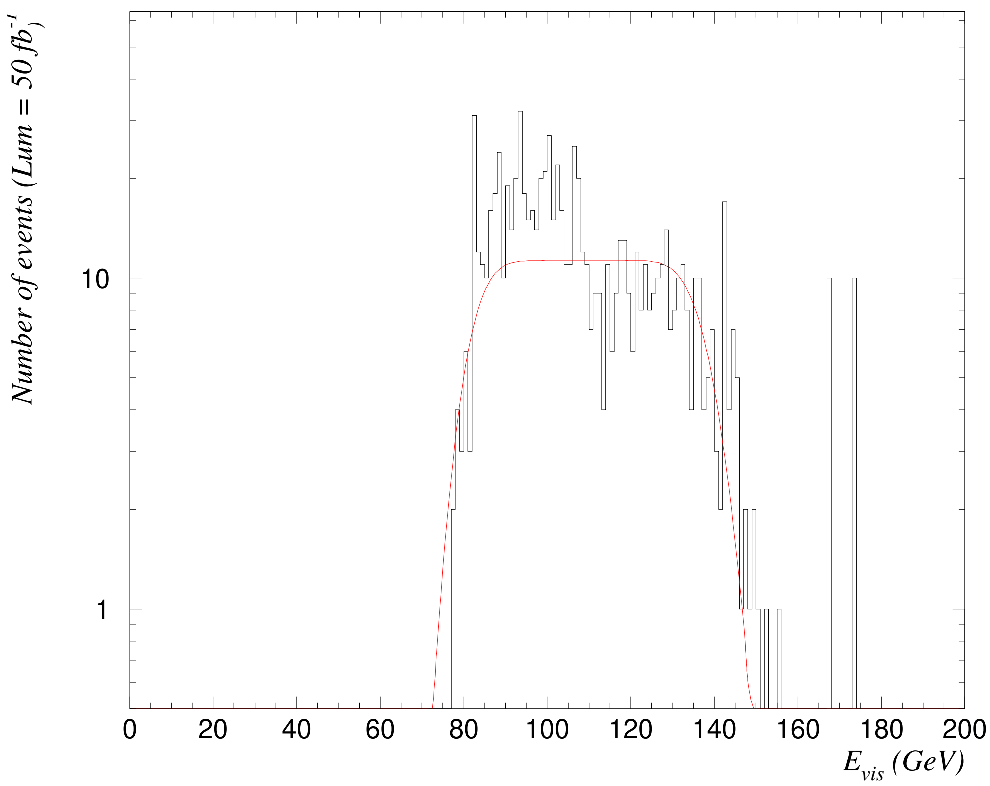

Figure 15: Sum of the Energy of jets associated with a W

shows the energy distribution for one of the $W^{\pm}$'s. Conservation of energy insists that the sum of the energy of the jets be equal to the energy of the $W^{\pm}$ which produced the jets. Therefore the maximum and minimum values for the energy of the $W^{\pm}$ correspond to the maximum and minimum end points of our histogram. The end points were found using a gaussian fit program to be:

$$E_{W,max} = 138.70 \pm 1.4 \text{ GeV}$$
$$E_{W,min} = 80.70 \pm 2.2 \text{ GeV}.$$

Using the input masses for point one and the mass of the $W^{\pm}$ in the equations derived in Appendix B we find that the correct values for $E_{W,max}$ and $E_{W,min}$ are:

$$E_{W,max} = 149.18 \text{ GeV}$$
$$E_{W,min} = 92.69 \text{ GeV}.$$

As you can see there is 7% discrepancy in our value for $E_{W,max}$ and a 13% discrepancy in our value for $E_{W,min}$. It is interesting to ask how much of an effect these discrepancies have on our final measurement of $M_{\tilde{\chi}_1^{\pm}}$ and $M_{\tilde{\chi}_1^0}$.

For the process, A $\Rightarrow$ B + C ($\tilde{\chi}_1^{\pm} \Rightarrow \tilde{\chi}_1^0 + W^{\pm}$), the error in our measurement of $M_A$is given by,

$$\delta M_A = \sqrt{\left(\frac{\partial M_A}{\partial E_{c,max}}\delta_{E_{c,max}}\right)^2 + \left(\frac{\partial M_A}{\partial E_{c,min}}\delta_{E_{c,min}}\right)^2}$$

Since $E_{c,max}$and $E_{c,min}$depend on the center of mass energy we can plot the δM_A as a function of $\sqrt{s}$ and see if there is an optimum energy for which to run the experiment. Using the results of Appendices A through D we plotted $\delta M_{\tilde{\chi}_1^{\pm}}$ versus the center of mass energy. Figure 16 shows these results. Note

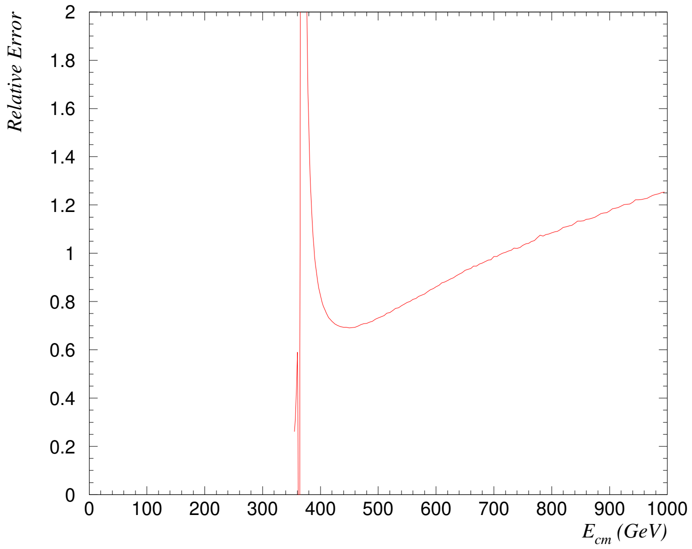

Figure 16: $\delta M_{\tilde{\chi}_1^{\pm}}$ versus $\sqrt{s}$ for the decay $\tilde{\chi}_1^{\pm} \Rightarrow \tilde{\chi}_1^0 + W^{\pm}$

that there is a minimum at $\sqrt{s} \sim 445$ GeV. This suggest that we can minimize our error by running the experiment at 445 GeV.

Using the formulas derived in the Appendix A,

$$M_{\tilde{\chi}_1^\pm} = \sqrt{\frac{(M_W^2 + E_{W,max}E_{W,min}) - \sqrt{(M_W^2 - E_{W,max}^2)(M_W^2 - E_{W,min}^2)}}{2(E_{W,max} + E_{W,min})^2/s}}$$

$$M_{\tilde{\chi}_1^0} = \sqrt{M_{\tilde{\chi}_1^\pm}^2 (1 - 2\frac{(E_{W,max} + E_{W,min})}{\sqrt{s}}) + M_W^2} ,$$

we find that the calculated masses for the $\tilde{\chi}_1^0$ and the $\tilde{\chi}_1^\pm$ are $M_{\tilde{\chi}_1^\pm} = 206$ GeV and $M_{\tilde{\chi}_1^0} = 108$ GeV. Because we used data from decays which had a combined mass of 80$\pm$5 GeV there is an uncertainty in the mass which must be taken into account. $|M_{\tilde{\chi}_1^\pm} - M_{\tilde{\chi}_1^\pm}(\Delta M_W)|_{max}$ is equal to 20 GeV for the values of ΔM_W from 75 to 85 GeV. Similarly we see that $|M_{\tilde{\chi}_1^0} - M_{\tilde{\chi}_1^0}(\Delta M_W)|_{max}$ is equal to 9 GeV for these same values of ΔM_W. So we see that,

$$M_{\tilde{\chi}_1^\pm} = 206 \pm 20 \text{ GeV}$$
$$M_{\tilde{\chi}_1^0} = 108 \pm 9 \text{ GeV}.$$

From table 2 one can see that the correct masses for point 1 are:

$$M_{\tilde{\chi}_1^\pm} = 175.4 \text{ GeV}$$
$$M_{\tilde{\chi}_1^0} = 86.1 \text{ GeV}.$$

We are approximately two standard deviations away from the input masses.

6 Conclusion

By using computer simulations our High Energy physics group has been conducting a study of how one might detect Supersymmetry in the lab environment. This paper looked at one of the five parameter points which have been chosen for this study. We have determined a set of cuts which increase the signal to background ratio dramatically, allowing one to see a clear signal of SUSY. During this process 80%[15] of the signal was lost but the background was virtually eliminated. This data was then used to obtain $E_{W,max}$ and $E_{W,min}$ in order to determine the masses of the Supersymmetric particles being produced. The calculated masses differed by approximately 20% from the input masses for this particular parameter set.

Supersymmetry would stop quadratic mass divergence in the scalar Higgs field and may possibly unify the strong and electroweak force at high energies. It has even been suggested that "dark matter" could be the LSP. For these reasons SUSY is an exciting theory in the world of high energy and particle physics and proof of its existence would dramatically improve our understanding of the particles which make up our world and the forces that cause them to interact.

[15] *See table 5*

Appendix A: The Endpoint Method

This section is a mathematical derivation of how to calculate the masses of the particles in a two body decay. We are concerned with the decay of the chargino where, $\tilde{\chi}_1^{\pm} \Rightarrow \tilde{\chi}_1^0 + W^{\pm}$. More generally this is just a two body decay, A $\Rightarrow$ B + C. In such a decay it is possible to find the masses of A and B if one knows the mass of C and the maximum and minimum energies of C in the lab frame.

In the center of mass of A,

$$\begin{aligned} E_{B,cm} &= E_{A,cm} - E_{C,cm} \; ...thus... \\ E^2_{B,cm} &= E^2_{A,cm} + E^2_{C,cm} - 2E_{A,cm}E_{C,cm}. \end{aligned}$$

Since the square of the energy four vector is invariant this equation becomes,

$$M_B^2 = M_A^2 + M_C^2 - 2M_A E_{C,cm}. \tag{A.1}$$

Solving for $E_{C,cm}$ gives,

$$E_{C,cm} = \frac{M_A^2 + M_C^2 - M_B^2}{2M_A}. \tag{A.2}$$

Now doing a Lorentz transformation into the lab frame we see that,

$$\begin{aligned} E_{C,lab} &= \gamma(E_{C,cm} - \beta p_{C,cm}\cos\theta) \; ...thus... \\ E_{c,max} &= \gamma(E_{C,cm} + \beta p_{C,cm}) \qquad (A.3) \\ E_{c,min} &= \gamma(E_{C,cm} - \beta p_{C,cm}). \qquad (A.4) \end{aligned}$$

Combining equations (A.3) and (A.4) we find that,

$$\begin{aligned} (E_{c,max} + E_{c,min}) &= 2\gamma E_{C,cm} \; ...thus... \qquad (A.5) \\ E^2_{C,cm} &= \frac{(E_{c,max} + E_{c,min})^2}{4\gamma^2} \qquad (A.6) \end{aligned}$$

By using the fact that $E^2 = p^2 + M^2$ we see that,

$$\begin{aligned} E_{c,max}E_{c,min} &= \gamma^2(E_{C,cm}^2 - \beta^2 p_{C,cm}^2) \\ &= \gamma^2(E_{C,cm}^2 - \beta^2(E_{C,cm}^2 - M_C^2)) \\ &= \gamma^2(1-\beta^2)E_{C,cm}^2 + \gamma^2\beta^2 M_C^2 \\ &= E_{C,cm}^2 + \gamma^2\beta^2 M_C^2 \end{aligned} \tag{A.7}$$

Equation (A.7) follows from the fact that $\gamma = 1/\sqrt{1-\beta^2}$. The center of mass frame of A is boosted by the velocity of particle A, v_A. Therefore if we define s to be the square of the center of mass energy of the collider, s $\equiv E_{cm}{}^2$, and noting that $E_{cm} = 2E_{A,cm}$ it follows that $E_{A,cm} = \sqrt{s}/2$. Now we can see that

$$\begin{aligned} \beta &\equiv \frac{p_{A,cm}}{M_A} \\ &= \frac{1}{E_{A,cm}}\frac{\sqrt{E_{A,cm}^2 - M_A^2}}{E_{A,cm}} \\ &= \sqrt{1-(\frac{M_A}{E_{A,cm}})^2} \\ &= \sqrt{1-4M_A^2/s} \end{aligned} \tag{A.8}$$

From equation (A.8) we now see that,

$$\gamma = \frac{1}{\sqrt{1-(1-4M_A^2/s)}} = \frac{\sqrt{s}}{2M_A} \tag{A.9}$$

Now by combining equations (A.6) through (A.9) we find that,

$$\begin{aligned} E_{c,max}E_{c,min} &= \frac{(E_{c,max} + E_{c,min})^2}{4\gamma^2} + \gamma^2\beta^2 M_C^2 \\ &= \frac{(E_{c,max} + E_{c,min})^2}{4s/4M_A^2} + \frac{s}{4M_A^2}(1-\frac{4M_A^2}{s})M_C^2 \ ...thus.. \\ M_A^2 E_{c,max}E_{c,min} &= M_A^4\frac{(E_{c,max} + E_{c,min})^2}{s} - M_A^2 M_C^2 + \frac{sM_C^2}{4} \end{aligned}$$

Which gives us a quadratic in M_A^2,

$$M_A^4 \frac{(E_{c,max} + E_{c,min})^2}{s} - M_A^2(M_C^2 + E_{c,max}E_{c,min}) + \frac{sM_C^2}{4} = 0 \quad \text{(A.10)}$$

Equation (A.10) is easily solved,

$$M_A^2 = \frac{(M_C^2 + E_{c,max}E_{c,min}) \pm \sqrt{K}}{2(E_{c,max} + E_{c,min})^2/s}$$

where let K is defined as,

$$\begin{aligned} K &\equiv (M_C^4 + 2M_C^2 E_{c,max}E_{c,min} + E_{c,max}^2 E_{c,min}^2) \\ &\qquad -4\frac{(E_{c,max}^2 + E_{c,min}^2 + 2E_{c,max}E_{c,min})}{s}\frac{sM_C^2}{4} \\ &= M_C^4 - M_C^2(E_{c,max}^2 + E_{c,min}^2) + E_{c,max}^2 E_{c,min}^2 \\ &= (M_C^2 - E_{c,max}^2)(M_C^2 - E_{c,min}^2) \end{aligned}$$

So we see that,

$$M_A^2 = \frac{(M_C^2 + E_{c,max}E_{c,min}) \pm \sqrt{(M_C^2 - E_{c,max}^2)(M_C^2 - E_{c,min}^2)}}{2(E_{c,max} + E_{c,min})^2/s}. \quad \text{(A.11)}$$

Appendix C explains how the kinematics of the event determine whether the + or the - sign is correct. We can now use the mass of A to find the mass of B. Using equations (A.1), (A.6) and (A.8) we see that,

$$\begin{aligned} M_B^2 &= M_A^2 + M_C^2 - 2M_A E_{C,cm} \\ &= M_A^2 + M_C^2 - 2M_A \frac{(E_{c,max} + E_{c,min})}{2\gamma} \\ &= M_A^2 + M_C^2 - 2M_A \frac{(E_{c,max} + E_{c,min})}{(2\sqrt{s}/2M_A)} \\ &= M_A^2 + M_C^2 - 2M_A^2 \frac{(E_{c,max} + E_{c,min})}{\sqrt{s}} \end{aligned} \quad \text{(A.12)}$$

So for the two body decay $A \Rightarrow B + C$, we have derived an equation which determines the masses of particles A and B from the mass of C and the maximum and minimum values of the energy of particle C in the lab frame.

Appendix B: Theoretical determination of $E_{c,max}$ and $E_{c,min}$

This is a derivation of the correct values for $E_{c,max}$and $E_{c,min}$. It is used to find the error in our measured values of $E_{c,max}$and $E_{c,min}$and in determining the $\pm$ in equation (A.11) is correct. First equations (A.2), (A.5) and (A.9) we see that,

$$\begin{aligned}
(E_{c,max} + E_{c,min}) &= 2\gamma E_{C,cm} \\
&= \sqrt{s}\,\frac{M_A^2 + M_C^2 - M_B^2}{2M_A^2} \\
&\equiv \sqrt{s}\,\zeta \\
&\equiv A
\end{aligned}$$

(where we have defined: $\zeta \equiv \frac{M_A^2 + M_C^2 - M_B^2}{2M_A^2}$),
and from equations (A.2), (A.7), (A.9), our definition of ζ and $\beta^2 = 1 - \gamma^{-2}$

we can see that,

$$\begin{aligned}
E_{c,max}E_{c,min} &= E_{C,cm}^2 + \gamma^2\beta^2 M_C^2 \\
&= M_A^2\zeta^2 - M_C^2 + \frac{sM_C^2}{4M_A^2} \\
&\equiv \eta + \frac{sM_C^2}{4M_A^2} \\
&\equiv B
\end{aligned}$$

(where we have defined $\eta = M_A^2\zeta^2 - M_C^2$).
Now if we use equations (B.1) and (B.2) we see that,

$$AE_{c,max} = (E_{c,max} + E_{c,min})E_{c,max} = E_{c,max}^2 + B$$

From the above equation and from the symmetry of the problem we can see that,

$$
\begin{aligned}
E_{c,max}^2 \;-\; AE_{c,max} \;+\; B \;&=\; 0 \\
E_{c,min}^2 \;-\; AE_{c,min} \;+\; B \;&=\; 0
\end{aligned}
$$

Using the quadratic equation and noting that $E_{c,max} \geq E_{c,min}$ gives us,

$$E_{c,max} = \frac{A + \sqrt{A^2 - 4B}}{2} \tag{B.1}$$

$$E_{c,min} = \frac{A - \sqrt{A^2 - 4B}}{2} \tag{B.2}$$

Appendix C: Determination of $\pm$

This section shows how the kinematics of the event determine whether the + or the - sign is correct in equation (A.11). As previously stated, we are interested in $\tilde{\chi}_1^\pm \Rightarrow \tilde{\chi}_1^0 + W^\pm$.

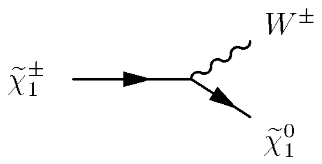

At threshold the $\tilde{\chi}_1^\pm$ is produced at rest in the lab frame. Conservation of momentum and energy then implies that the $W^\pm$ and the $\tilde{\chi}_1^0$ are produced opposite directions with equal energy. Since $M_{\tilde{\chi}_1^\pm}$ is greater than twice $M_{W^\pm}$ the $W^\pm$ will have some amount of kinetic energy. However, if the $\tilde{\chi}_1^\pm$ is moving in the lab frame and the $W^\pm$ is produced in the opposite direction of the $\tilde{\chi}_1^\pm$ the $W^\pm$ may be produced at rest in the lab. Figure 17 is a plot of

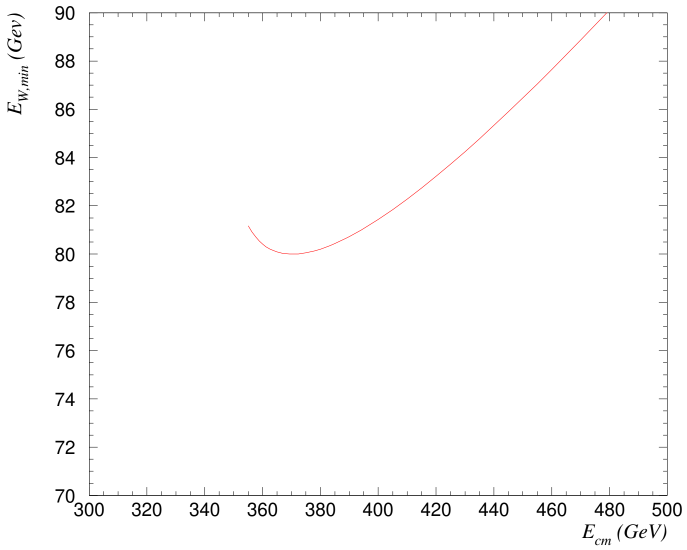

Figure 17: $E_{W^\pm,min}$ versus $\sqrt{s}$ for the decay $\tilde{\chi}_1^\pm \Rightarrow \tilde{\chi}_1^0 + W^\pm$

$E_{W^\pm,min}$ versus $\sqrt{s}$ for the decay $\tilde{\chi}_1^\pm \Rightarrow \tilde{\chi}_1^0 + W^\pm$ (Point 1).

When $E_{W,min}$ is a minimum, $E_{W,min} = M_{W^\pm}$, the discriminant in equation (A.11) is zero. We will call this point $E_{critical}$. For the case where $E_W = E_{W,min}$, if $\sqrt{s}$ is less than $E_{critical}$ the $W^\pm$ moves in the opposite direction as the $\tilde{\chi}_1^\pm$ in the lab and the + sign in equation (A.11) is correct. If however, $E_W = E_{W,min}$ and $\sqrt{s}$ is greater than $E_{critical}$ the $W^\pm$ moves in the same direction of the $\tilde{\chi}_1^\pm$ in the lab and the - sign is correct. From figure 17 you can see for Point 1, $\tilde{\chi}_1^\pm \Rightarrow \tilde{\chi}_1^0 + W^\pm$, this critical point occurs at $\sqrt{s} = 370$ GeV.

We came to this conclusion by plugging the correct values of $E_{c,max}$and $E_{c,min}$, as derived in Appendix B, back into equation (A.11) and seeing which sign gave us the correct masses.

Appendix D: Dependence of the Error on the Center of Mass Energy

We know that,

$$\delta M_A^2 \;=\; \sqrt{(\frac{\partial M_A^2}{\partial E_{c,max}}\delta_{E_{c,max}})^2 \;+\; (\frac{\partial M_A^2}{\partial E_{c,min}}\delta_{E_{c,min}})^2}$$

or that,

$$\delta M_A \;=\; \frac{\sqrt{(\frac{\partial M_A^2}{\partial E_{c,max}}\delta_{E_{c,max}})^2 \;+\; (\frac{\partial M_A^2}{\partial E_{c,min}}\delta_{E_{c,min}})^2}}{2M_A}. \tag{D.1}$$

From equation (A.11) we see that,

$$\frac{\partial M_A^2}{\partial E_{c,max}} \;=\; \frac{E_{c,min} \;\mp\; E_{c,max}\;(M_C^2 - E_{c,min}^2)/\sqrt{(M_C^2 - E_{c,max}^2)(M_C^2 - E_{c,min}^2)}}{2(E_{c,max} +\; E_{c,min})^2/s}$$
$$-\;\frac{(M_C^2 +\; E_{c,max}E_{c,min}) \pm \sqrt{(M_C^2 - E_{c,max}^2)(M_C^2 - E_{c,min}^2)}}{(E_{c,max} +\; E_{c,min})^3/s}$$

If we let $P \;\equiv\; (E_{c,max} \;+\; E_{c,min})$ and let $Q \;\equiv\; (M_C^2 - E_{c,max}^2)(M_C^2 - E_{c,min}^2)$ and do a little simplifying, we find that,

$$\frac{\partial M_A^2}{\partial E_{c,max}} \;=\; \frac{s}{2\;P^3}\Bigg\{\;E_{c,min}(E_{c,min} \;-\; E_{c,max}) \;-\; 2M_C^2$$
$$\mp\sqrt{Q}\left(2 \;+\; \frac{E_{c,max}(M_C^2 - E_{c,min}^2)P}{Q}\right)\Bigg\},$$

and from the symmetry in the equation for $M_A$we find that,

$$\frac{\partial M_A^2}{\partial E_{c,min}} \;=\; \frac{s}{2\;P^3}\Bigg\{\;E_{c,max}(E_{c,max} \;-\; E_{c,min}) \;-\; 2M_C^2$$
$$\mp\sqrt{Q}\left(2 \;+\; \frac{E_{c,min}(M_C^2 - E_{c,max}^2)P}{Q}\right)\Bigg\}.$$

(The $\mp$ is determined as shown in Appendix C).

We plotted the δM_A, equation (D.1), using these derivatives, the theoretical values for $E_{c,max}$ and $E_{c,min}$ derived in Appendix B and the standard deviation of the mean,

$$\begin{aligned} \delta_{E_{c,max/min}} &= \sigma/\sqrt{Number\ of\ Events\ near\ edge} \\ &= \sigma/\sqrt{2 * \sigma * \rho}. \end{aligned}$$

Here σ is the resolution of the detector,

$$\sigma = E_{c,max/min}(0.12 + \frac{0.01}{\sqrt{E_{c,max/min}}}),$$

and the density, assuming a square distribution, is,

$$\begin{aligned} \rho &= \frac{Number\ of\ Events}{\Delta E} \\ &= \frac{Luminosity * Cross\ Section * (\%\ of\ Signal\ left\ after\ cuts)}{E_{c,max} - E_{c,min}} \end{aligned}$$

Figure 16 shows these results for $\tilde{\chi}_1^{\pm} \Rightarrow \tilde{\chi}_1^0 + W^{\pm}$. In Figure 16 we assumed that the % of the signal left after cuts is constant, 20% (See table 5).